

Pull-in instability of parallel-plate electrostatic microactuators under a combined variable charge and voltage configuration

C. Son and B. Ziaie

Citation: [Applied Physics Letters](#) **92**, 013509 (2008); doi: 10.1063/1.2832770

View online: <http://dx.doi.org/10.1063/1.2832770>

View Table of Contents: <http://scitation.aip.org/content/aip/journal/apl/92/1?ver=pdfcov>

Published by the [AIP Publishing](#)

Articles you may be interested in

[A continuum model for the static pull-in behavior of graphene nanoribbon electrostatic actuators with interlayer shear and surface energy effects](#)

[J. Appl. Phys.](#) **113**, 153512 (2013); 10.1063/1.4800543

[Frequency-dependent stability of parallel-plate electrostatic actuators in conductive fluids](#)

[Appl. Phys. Lett.](#) **96**, 203505 (2010); 10.1063/1.3389491

[Theoretical dynamic response of electrostatic parallel plate](#)

[Appl. Phys. Lett.](#) **91**, 183513 (2007); 10.1063/1.2803323

[Suppression of the pull-in instability for parallel-plate electrostatic actuators operated in dielectric liquids](#)

[Appl. Phys. Lett.](#) **88**, 034105 (2006); 10.1063/1.2165282

[A general relation between the ranges of stability of electrostatic actuators under charge or voltage control](#)

[Appl. Phys. Lett.](#) **82**, 302 (2003); 10.1063/1.1536251

The image shows the cover of the journal Applied Physics Reviews. It features a blue and orange color scheme with a molecular structure in the background. The text 'AIP Applied Physics Reviews' is at the top left. The main title 'NEW Special Topic Sections' is in large white letters. Below it, 'NOW ONLINE' is in orange, followed by 'Lithium Niobate Properties and Applications: Reviews of Emerging Trends' in white. The AIP logo and 'Applied Physics Reviews' are at the bottom right.

NEW Special Topic Sections

NOW ONLINE
Lithium Niobate Properties and Applications:
Reviews of Emerging Trends

AIP Applied Physics
Reviews

Pull-in instability of parallel-plate electrostatic microactuators under a combined variable charge and voltage configuration

C. Son and B. Ziaie^{a)}*School of Electrical and Computer Engineering, Purdue University, W. Lafayette, Indiana 47907, USA*

(Received 20 October 2007; accepted 17 December 2007; published online 8 January 2008)

In this letter, we present a theoretical analysis of pull-in instability of parallel-plate electrostatic microactuators under a combined variable charge and voltage configuration. This occurs in parallel plate capacitors partially filled with a charged dielectric (electret) where the plates are connected together through an impedance. Our results demonstrate the possibility of achieving full range motion under certain conditions. For Teflon® electrets much thinner than the air gap; the maximum traveling distance is similar to the voltage controlled electrostatic actuators ($\text{gap}/3$), whereas for electrets four times thicker than the initial gap the maximum traveling distance can approach 100% of the gap. © 2008 American Institute of Physics. [DOI: 10.1063/1.2832770]

Due to their favorable scaling properties in the micro-domain, electrostatic actuators play an important role in many microelectromechanical systems transducers.¹ It is a common knowledge that under constant voltage configuration, the pull-in instability limits the traveling distance to one-third of the gap. Such instability, however, does not exist under a constant charge configuration.² An important group of applications does not fit strictly between these two ideal cases. These include microdevices in which the capacitor gap is partially filled with a charged dielectric (i.e., electret). Micromachined electret microphones, electret power scavengers, and electret-based wireless microionization chambers are some examples of such applications.^{3–6} In these cases, the plates of the capacitor are typically connected via a resistor (e.g., microphones) or an inductor (e.g., wireless dosimeters). For such configurations in which both the surface charge and the voltage between the plates are variable, an electromechanical stability analysis has not been attempted.

Figure 1 shows a schematic of such a configuration. An electret layer is placed on the fixed bottom electrode and a top electrode on a movable membrane is connected to the bottom electrode via an impedance (for the purpose of this discussion the nature of the impedance is irrelevant and the two plates can be considered shorted together). The top membrane is supported by the spring with spring constant k , enabling vertical movement. Electrostatic force pulling the membrane in a simple voltage controlled configuration can be given by $F_e = \epsilon_0 A V^2 / 2(x_0 - x)^2$ in which A is the area of the membrane, V is the voltage applied, x_0 is the initial air gap, x is the membrane deflection, and ϵ_0 is the gap permittivity (air in this case). Pull-in instability (i.e., snap through) occurs at a deflection of $x = x_0/3$.²

When the membrane is controlled by surface charge, the electrostatic force can be expressed as $F_e = \sigma^2 / 2\epsilon_0$, where σ is the surface charge density on the plates. In this case, the snap through does not happen since the electrostatic force does not have a dependence on the distance between the charged plates. To find the electric force applied on the movable membrane shown in Fig. 1, the electric potential energy stored between the membrane and the bottom electrode can be calculated by the volume integral of the electric energy

density in the capacitive structure due to the charge on the electret surface. The electric field in the air gap and inside the electret can be described by the following:⁷

$$\mathbf{E}_{\text{airgap}} = \frac{\sigma}{\epsilon_0} \frac{1}{\left(1 + \frac{d_{\text{air}}}{d_{\text{electret}}} \epsilon_{\text{electret}}\right)} \hat{n}, \quad (1)$$

$$\mathbf{E}_{\text{electret}} = \frac{\sigma}{\epsilon_0} \frac{1}{\left(\frac{d_{\text{electret}}}{d_{\text{air}}} + \epsilon_{\text{electret}}\right)} (-\hat{n}), \quad (2)$$

where σ is the surface charge density of the electret, A is the area of the membrane, $\epsilon_{\text{electret}}$ is the dielectric constant of the electret, ϵ_0 is the permittivity of free space, and d_{air} and d_{electret} are the air gap and electret thicknesses, respectively.

The existence of an electric field in the air gap is due to the charge distribution between the top and the bottom plates once the electret is placed inside the capacitor. Although the total positive and negative charges are equal, their distribution between the plates depends on the gap size and electret properties (thickness and dielectric constant). Figure 2 shows the charge distribution between the two plates (area of 4 mm²) as a function of air gap for a 25 μm Teflon® electret having a surface charge density of 800 $\mu\text{C}/\text{m}^2$. As can be seen, at small air gaps, the majority of the charge is on the top plate and as the gap increases, more of the charge relocates to the bottom plate. The electric field in the air gap also corresponds to the charge distribution with the field being stronger at smaller gaps.

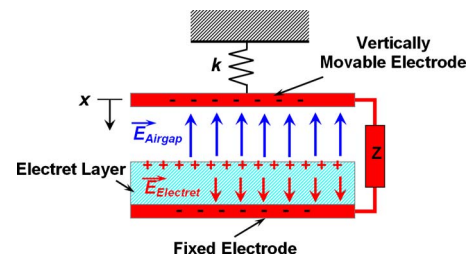


FIG. 1. (Color online) Electric field and charge distribution in a parallel plate capacitor partially filled with an electret.

^{a)}Electronic mail: bziaie@purdue.edu. Tel.: +1 765-494-0725.

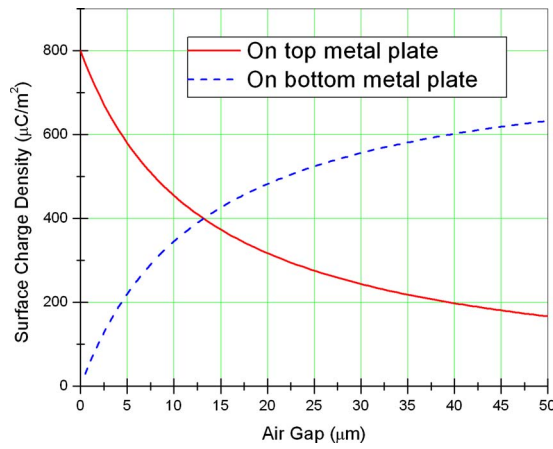


FIG. 2. (Color online) Surface charge distribution between two plates of a capacitor (area of 4 mm²) partially filled with a 25 μm thick Teflon® electret having a surface charge density of 800 C/m² as a function of air gap.

The integral of the electric energy density ($1/2\epsilon E^2$) over the total volume of the space between two electrodes can be given by (fringing electric fields are ignored in this calculation)

$$U = \frac{1}{2} \frac{\sigma^2 A}{\epsilon_0} \left(\frac{1}{d_{\text{air}}} + \frac{\epsilon_{\text{electret}}}{d_{\text{electret}}} \right)^{-1}. \quad (3)$$

The electrostatic force exerted on the movable membrane in Fig. 1 can thus be calculated by taking the derivative of the stored electrostatic energy with respect to the membrane displacement,

$$F_e = \frac{1}{2} \frac{\sigma^2 A}{\epsilon_0} \frac{1}{\left(1 + \epsilon_{\text{electret}} \frac{d_{\text{air}}}{d_{\text{electret}}} \right)^2}. \quad (4)$$

Assuming a linear membrane restoring force $F_r = -kx$, the electric force deflects the membrane up to the point where F_e and restoring force F_r balance each other yielding

$$kx = \frac{1}{2} \frac{\sigma^2 A}{\epsilon_0} \frac{1}{\left(1 + \epsilon_{\text{electret}} \frac{x_0 - x}{d_{\text{electret}}} \right)^2}, \quad (5)$$

where d_{air} is replaced by the initial air gap x_0 minus the deflection x . This force balance equation can be solved for surface charge density σ .

$$\sigma = \sqrt{2 \frac{k\epsilon_0}{A} x \left(1 + \epsilon_{\text{electret}} \frac{x_0 - x}{d_{\text{electret}}} \right)^2} \quad (6)$$

shows the relationship between the membrane deflection (x) and the surface charge density (σ). Figure 3(a) shows membrane deflection versus surface charge density for a capacitor with a plate area of 4 mm² and a total gap of 50 μm. The electret thickness is assumed to be 1 μm having a dielectric constant of ~ 2 (Teflon®). As can be seen, the membrane deflection increases with the surface charge density. However, there is a maximum point for the surface charge density above which the membrane deflection is limited by pull-in instability. For example, for a surface charge density of 780 μC/m², the membrane deflection is limited to 16 μm when spring constant k is 2 N/m. Above this value, the membrane is pulled down due to an increase in the electric field and resulting elastic instability (*pull-in charge density*).

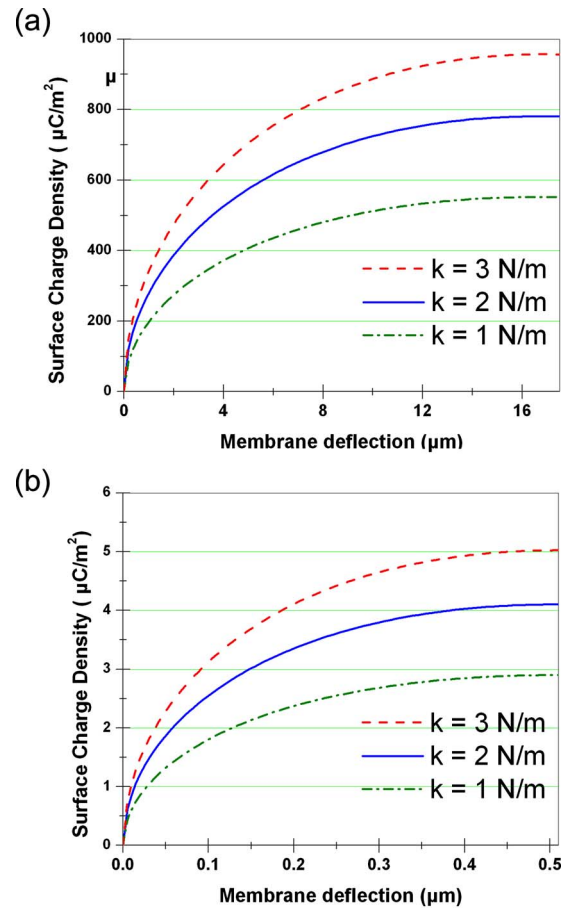


FIG. 3. (Color online) Membrane deflection curves vs surface charge density for (a) a membrane with ($A=4$ mm², $\epsilon_{\text{electret}}=1.9$, $d_{\text{electret}}=1$ μm, $x_0=50$ μm) and (b) a membrane with ($A=4$ mm², $\epsilon_{\text{electret}}=1.9$, $d_{\text{electret}}=1$ μm, $x_0=1$ μm).

To calculate the maximum deflection point, we take the first derivative on surface charge density, $d\sigma/dx=0$. The maximum deflection before the elastic instability can be calculated

$$x_{\text{max}} = \left(\frac{d_{\text{electret}}}{3\epsilon_{\text{electret}}} + \frac{x_0}{3} \right). \quad (7)$$

If the air gap x_0 is much larger than the electret thickness d_{electret} (e.g., bulk micromachined structures in which the two plates are flip chip bonded) the first term of Eq. (7) can be neglected. Therefore, $x_{\text{max}} \approx x_0/3$, which shows the same maximum deflection point as the voltage controlled membrane deflection. If x is replaced by $x_{\text{max}} \approx x_0/3$ in Eq. (6), one yields

$$\sigma_{\text{pull-in}} = \sqrt{2 \frac{k\epsilon_0}{A} \frac{x_0}{3} \left(1 + \epsilon_{\text{electret}} \frac{2x_0}{3d_{\text{electret}}} \right)^2}, \quad (8)$$

which shows the pull-in charge density associated with the maximum membrane deflection. If surface charge density is larger than this value, the membrane will collapse on the electret layer.

Figure 3(b) shows membrane deflection versus surface charge density for a capacitor with a plate area of 4 mm² and a total gap of 2 μm of which 1 μm is filled with Teflon® electret. This represents a situation in which the electret thickness is comparable to the air gap (e.g., surface micro-machined structures with a narrow gap). As can be seen, the

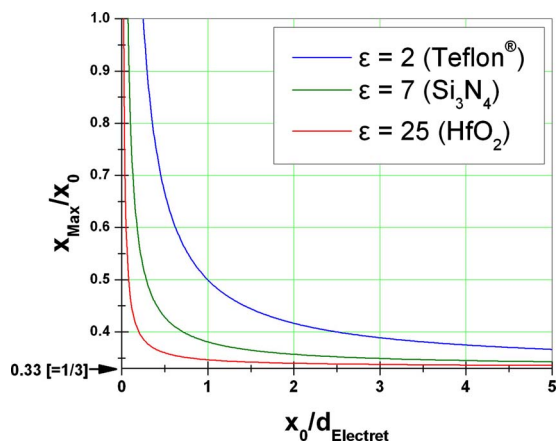


FIG. 4. (Color online) Normalized maximum membrane deflection vs the ratio of initial air gap to the electret layer thickness for several dielectrics.

membrane in this case can deflect up to 50% of its initial gap ($0.5 \mu\text{m}$) before snap through occurs. Also, for the same amount of deflection relative to the initial gap size, one needs two orders of magnitude lower surface charge density, if 50% of the gap is filled with electret. This is beneficial for sensing applications, since the sensitivity of parallel plate capacitive sensor increases by reducing the gap (at the expense of dynamic range). In situations for which a larger dynamic range is required, one can increase both the electret thickness and gap size simultaneously and still achieve a larger range of motion.

Figure 4 shows x_{max}/x_0 versus x_0/d_{electret} for a several dielectrics (i.e., Teflon®, silicon nitride, and hafnium oxide; chosen to represent a range of dielectric constants). As can be seen, for Teflon® with a $x_0/d_{\text{electret}}=0.25$, the maximum traveling distance is equal to the full gap thickness, whereas for a large $x_0/d_{\text{electret}} (>5)$ the membrane snaps through at

1/3 of the gap. Other dielectrics show a similar hyperbolic trend with the x_0/d_{electret} transitions happening at different points (the larger the dielectric constant the smaller the x_0/d_{electret} required for snap through or full-range motion with sharper transition behavior). Hence, depending on the electret dielectric constant and x_0/d_{electret} the pull-in behavior of a combined variable charge and voltage controlled micro-actuator can be anywhere between the ideal voltage and charge controlled configurations. This adds a unique control parameter in applications requiring full range motion across the gap.

In conclusion, we presented theoretical analysis of pull-in instability of parallel-plate electrostatic microactuators under a combined variable charge and voltage configuration. In spite of its important applications in electret-based microphones, power scavengers, and wireless microionization dosimeters, electromechanical analysis of its stability had not been attempted before. Our results demonstrate the possibility to achieve a full range motion under certain conditions (i.e., electret thickness and dielectric constant). For electrets much thinner than the air gap, the maximum traveling distance is similar to the voltage controlled electrostatic actuators (gap/3), whereas for thicker electrets the maximum traveling distance can approach 100% of the gap.

¹W. S. N. Trimmer, *Sens. Actuators* **19**, 267 (1989).

²S. D. Senturia, *Microsystem Design* (Kluwer, Boston, 2001), pp. 130–137.

³W. H. Hsieh, T. Y. Hsu, and Y. C. Tai, *Proceedings of the International Conference on Solid-State Sensors and Actuators*, 1997 (unpublished), pp. 425.

⁴F. Peano and T. Tambosso, *J. Microelectromech. Syst.* **14**, 429 (2005).

⁵C. Son and B. Ziaie, *IEEE Electron Device Lett.* **27**, 884 (2006).

⁶T. Tsutsumino, Y. Suzuki, N. Kasagi, and Y. Sakane, *Proceedings of the 19th IEEE International Conference on Micro Electro Mechanical Systems*, Istanbul, 2006 (unpublished), pp. 98–101.

⁷G. M. Sessler and M. G. Broadhurst, *Electrets* (Springer, Berlin, 1980), pp. 13–20.